CrossMark

ORIGINAL PAPER

Age and petrogenesis of late Paleozoic granites from the northernmost Alxa region, northwest China, and implications for the tectonic evolution of the region

Wen Zhang[1,2,3] · Victoria Pease[3] · Qingpeng Meng[2] · Rongguo Zheng[1] · Tairan Wu[2] ·
Yan Chen[2] · Lisheng Gan[2]

Abstract The Wudenghan, Huhetaoergai and Zhuxiaobuguhe plutons, northern Alxa region, in the southern Central Asia Orogenic Belt are dated by U–Pb zircon to 383 ± 3, 356 ± 3 and 286 ± 2 Ma, respectively. The late Devonian Wudenghan monzogranite, a highly fractionated I-type granite with $\varepsilon_{Nd}(t)$ (−0.2 to −0.1) and very low $(^{87}Sr/^{86}Sr)_t$ (0.704719–0.706113), is from mantle-derived magmas and shows volcanic arc characteristics. The early Carboniferous Huhetaoergai granodiorite with medium-K calc-alkaline peraluminous characteristics represents a volcanic arc granite generated from partial melting of lower continental crust combined with mantle-derived input. The early Permian Zhuxiaobuguhe pluton, an unfractionated calc-alkaline granodiorite with moderately low $\varepsilon_{Nd}(t)$ (−2.0 to −1.1) and low $(^{87}Sr/^{86}Sr)_t$ (0.708370–0.708462), was likely derived from partial melting of the mafic lower crust of a paleovolcanic arc and represents a post-collisional granite. Our revised tectonic evolution of the region includes (1) northward subduction of the oceanic crust represented by the Engger Us Ophiolitic Belt and formation of the late Devonian Wudenghan monzogranite, (2) northward subduction of the ocean between the Huhetaoergai and Zhusileng tectonic zones and the formation of the Huhetaoergai volcanic arc granite during the early Carboniferous and (3) the emplacement of the Zhuxiaobuguhe pluton in the early Permian during post-collisional extension.

Keywords Granite · Alxa · Central Asia Orogenic Belt · Paleozoic · Tectonics

✉ Tairan Wu
trwupku@163.com

1 Institute of Geology, Chinese Academy of Geological Sciences, Beijing 100037, China

2 Laboratory of Orogenic Belts and Crustal Evolution, Ministry of Education, School of Earth and Space Sciences, Peking University, Beijing 100871, China

3 Department of Geological Sciences, Stockholm University, 106 91 Stockholm, Sweden

Introduction

The northern Alxa region is located west of Inner Mongolia, China and links the central part of the southern Central Asia Orogenic Belt (CAOB) to its eastern and western parts (Fig. 1a, b). This is also where the North China Plate, the Tarim Plate and/or the Kazakhstan Plate meet (Fig. 1b; Wang et al. 1994; Wu et al. 1998). Its evolution is related to the development of the Paleo-Asian Ocean and its continental margins (Kröner et al. 2012, 2014; Şengör et al. 1993; Windley et al. 2007; Wilhem et al. 2012; Xiao et al. 2009a, b, 2013). The geological evolution of the area is so complicated that the relationships between the three plates and their Paleozoic evolution remain highly controversial (Wang et al. 1994; Wu et al. 1998; Zheng et al. 2014). Three important ophiolitic belts or sutures are reported in the northern Alxa region (Fig. 1c). From north to south, they include the Yagan Suture, the Engger Us Ophiolitic Belt and the Qagan Qulu Ophiolitic Belt (Wang et al. 1994; Wu and He 1992; Wu et al. 1998). The Engger Us Ophiolitic Belt is regarded as the suture between the North China Plate and the Tarim Plate (Wang et al. 1994; Wu and He 1992; Wu et al. 1998) or the major suture between the northern margin of the Alxa block (NMAB) and the CAOB (Zheng et al. 2014). The NMAB is usually considered to
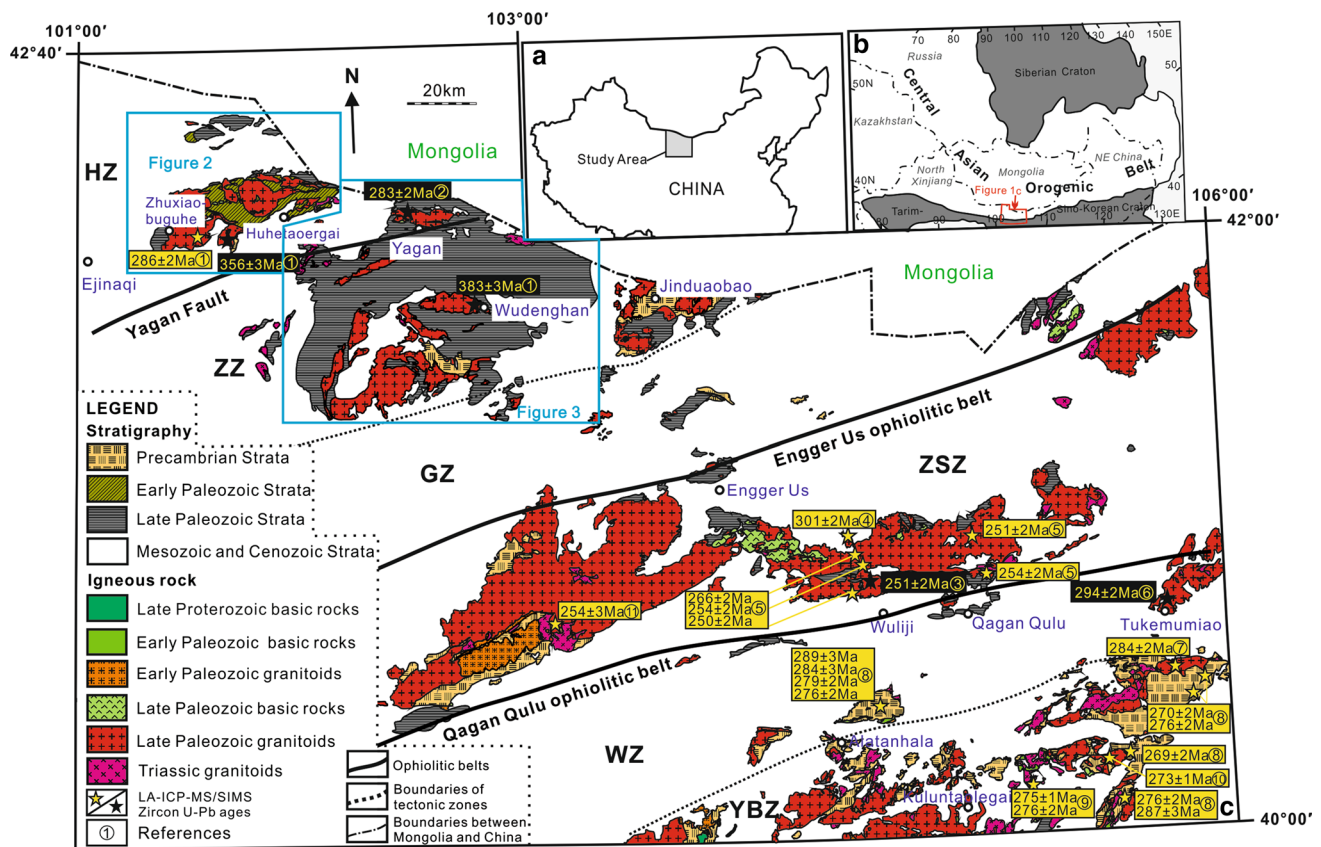
Fig. 1 a The northern Alxa region in China. **b** The northern Alxa region in the Central Asian Orogenic Belt (after Jahn et al. 2000); CAOB is the white area. **c** Simplified geological map of the northern Alxa region (after BGGP 1979, 1980, 1981a, b; BGIMAR 1980; BGNHAR 1976, 1980a, b, c, d, 1982a, b). Six tectonic zones from north to south: *HZ* Huhetaoergai zone, *ZZ* Zhusileng zone, *GZ* Guaizihu zone, *ZSZ* Zongnaishan–Shalazhashan zone, *WZ* Wuliji zone, *YBM* Yabulai-Bayinnuoergong zone. References for age data: 1 = this study; 2 = Zheng et al. (2013); 3 = Zhang et al. (2013a); 4 = Yang et al. (2014); 5 = Shi et al. (2014); 6 = Zhang (2013); 7 = Shi et al. (2012); 8 = Geng and Zhou (2012); 9 = Zhang et al. (2013b); 10 = Zhang et al. (2012); 11 = Ran et al. (2012)

be the western part of the North China Plate (Zhao et al. 2005), but in recent years many authors have suggested that the Alxa Block is not a part of the North China Craton (e.g., Dan et al. 2014; Zhang et al. 2011). The timing of obduction of the Engger Us Ophiolitic Belt and the Qagan Qulu Ophiolitic Belt has not been confirmed (Wang et al. 1994; Wu and He 1993; Zheng et al. 2014), and consequently, the timing of ocean closure represented by them remains controversial.

Most of the igneous rocks in the northern Alxa region are granites ranging from Precambrian to Mesozoic in age (Geng et al. 2002; Shi et al. 2014; Wang et al. 1994; Zhang et al. 2013a; Zheng et al. 2013; Yang et al. 2014). Due to the remote environment and tough working conditions, few granites north of the Engger Us Ophiolitic Belt are well studied, which would help to constrain the tectonic interpretation of the northern Alxa region (Wang et al. 1994; Zheng et al. 2013). We present new geochronological and geochemical data from three late Paleozoic granitic plutons in the west of the Huhetaoergai, the Zhuxiaobuguhe

and Wudenghan areas (Figs. 2, 3). These data constrain their ages, relationship and petrogenesis and also facilitate our understanding of the adjacent ophiolitic belts and their relationship to the late Paleozoic tectonic evolution of the northern Alxa region.

Geological background

Tectonic zones

Six tectonic zones are delimited in the northern Alxa region (Fig. 1c). From north to south, they are the Huhetaoergai, Zhusileng, Guaizihu, Zongnaishan–Shalazhashan, Wuliji and Yabulai-Bayinnuoergong tectonic zones (Wu et al. 1998; Wang et al. 1994; Zhang et al. 2013a). The last unit is interpreted to belong to the northern margin of the Alxa block, whereas the others belong to the CAOB (Shi et al. 2014; Wang et al. 1994; Zhang et al. 2013a; Zheng et al. 2014; Fig. 1). Together the latter three zones comprise a
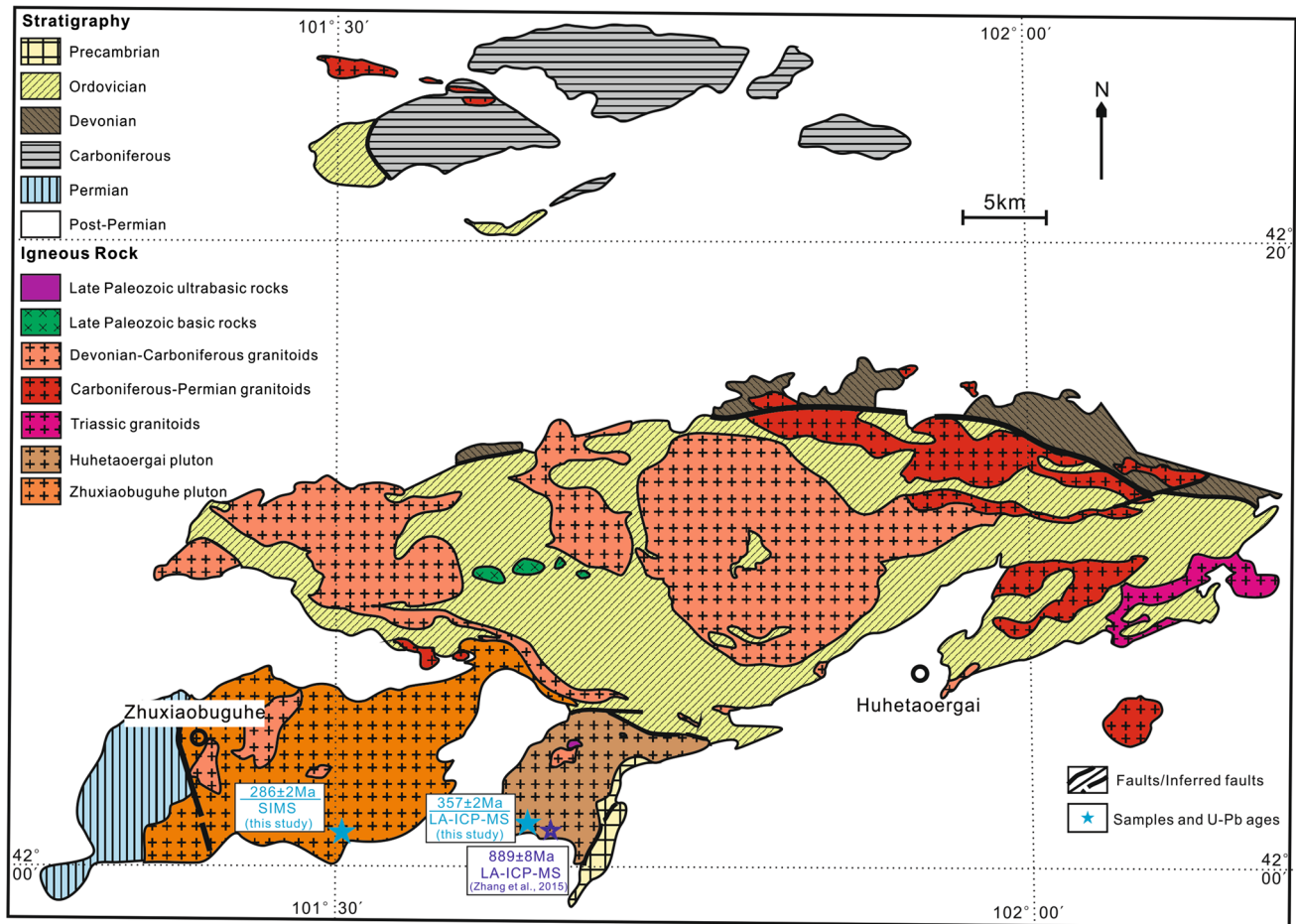
Fig. 2 Huhetaoergai and Zhuxiaobuguhe plutons, northern Alxa region (after BGGP 1980, 1981a)

complete trench-arc-basin system of Late Paleozoic age with the ocean represented by the Engger Us Ophiolitic Belt and the back-arc basin represented by the Qagan Qulu Ophiolitic Belt [for more details about the ophiolitic belts, see Zheng et al. (2014)]. The Wuliji granite in the Zongnaishan–Shalazhashan tectonic zone represents the mature arc of this system, similar to today's Japan island arc (Feng et al. 2013; Wang et al. 1994; Zhang et al. 2013a). The Qagan Qulu Ophiolitic Belt is considered to be the suture formed by the closure of the back-arc basin in the late Paleozoic (Wu and He 1992, 1993; Wu et al. 1998; Zheng et al. 2014).

The three northern zones of the CAOB are less studied. The Huhetaoergai tectonic zone is argued to be a volcanic arc developed on oceanic crust preserved when an ocean closed during the late Silurian–Devonian (Wang et al. 1994) or Permian (Wu et al. 1998). The passive continental margin represented by the Zhusileng and Guaizihu tectonic zones became an active continental margin in the end of the early Paleozoic and was under extension during the Carboniferous–Permian (Wang et al. 1994; Wu et al. 1998).

The Yagan Suture is considered to be an important boundary separating strata of different affinities. Rocks in the fault zone are highly fragmented and some ultramafic rocks are present (Wang et al. 1994; Wu et al. 1998; Fig. 1c), but no other ophiolitic components have been recognized so far.

Precambrian strata in the Huhetaoergai and Zhusileng tectonic zones

In the Huhetaoergai tectonic zone, Mesoproterozoic (Stenian–Estasian) strata in the west of the Western Huhetaoergai pluton are the only Precambrian strata exposed (Fig. 2). It consists of sandstone, thick marble, some silicalite and slate; the base contains purple-red sandstone with fine conglomerate (BGGP 1980). Paleoproterozoic–Neoproterozoic strata are found in the Zhusileng tectonic zone (Fig. 3). A widely distributed early Paleoproterozoic marine regression sedimentary sequence in the Jindouaobao area includes from bottom to top magnesium carbonates, intermediate-acidic volcanic rocks
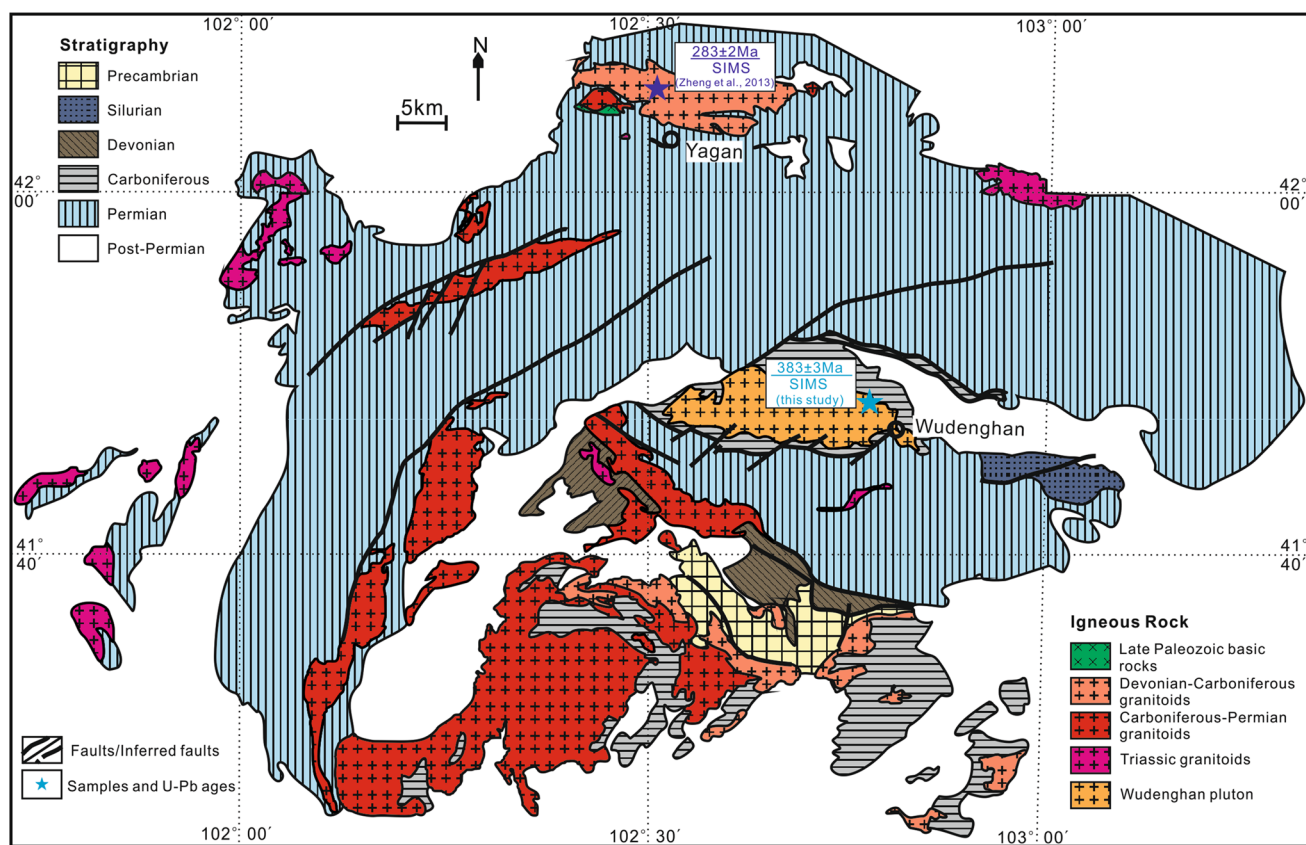
Fig. 3 Wudenghan pluton, northern Alxa region (after BGGP 1981a, b; BGNHAR 1982a)

and clastic rocks (BGNHAR 1982a). Mesoproterozoic (Stenian–Estasian) strata are composed of metasiltstone in the lower and upper parts and carbonate in the middle; they are in fault contact and only exposed south of the Wudenghan area (BGGP 1981a). Minor late Paleoproterozoic–early Neoproterozoic (Statherian–Calymmian) neritic carbonates and black siliceous rocks, early Neoproterozoic (Tonian) siliceous dolomites and late Neoproterozoic (Cryogenian) glacial till (ca. 90 m) also occur in the Zhusileng tectonic zone (BGNHAR 1982a; Wang et al. 1994).

Paleozoic strata in the Huhetaoergai and Zhusileng tectonic zones

In the Huhetaoergai tectonic zone, Middle Ordovician strata are the only early Paleozoic strata exposed (Fig. 2). They are divided into lower, middle and upper parts: neritic intermediate volcanic rocks, clastic rocks and intermediate-acidic volcanic rocks, respectively (BGGP 1980). The Middle Ordovician strata are not exposed in the Zhusileng tectonic zone (Figs. 1c, 3). However, it preserves a continuous sedimentary record from Cambrian to Middle Silurian (Wang et al. 1994). Thick carbonates, silicalites and flysch

reflect a passive continental margin environment (Wang et al. 1994; Wu et al. 1998).

The Lower Devonian to Lower Carboniferous-lower part of Upper Carboniferous strata are dominated by littoral–neritic volcanic and clastic rocks in the Huhetaoergai tectonic zone (Fig. 2). Devonian strata are well developed in the Zhusileng tectonic zone. Its western part mainly consists of neritic clastic rocks and biohermal limestone, and its eastern part is composed of unstable neritic volcanic and clastic rocks. In the Wudenghan area, an early Carboniferous anticline folds gray-green graywacke and feldspathic graywacke with interlayered gray-green andesitic basalts (Fig. 3; BGGP 1981a). Lower Carboniferous strata including neritic volcanic and clastic rocks also occur in the Zhusileng tectonic zone. Permian strata are widely distributed in both the Huhetaoergai and Zhusileng tectonic zones (Fig. 1c; BGGP 1980, 1981a; BGNHAR 1982a). They lie unconformably on Carboniferous strata (Wang et al. 1994). Lower Permian strata in the Huhetaoergai tectonic zone comprise clastic rocks in the lower part and volcanic rocks with graywacke in the upper part, indicating an unstable neritic environment (BGGP 1980, 1981a). It coincides with the widespread Lower Permian Shuangbaotang Formation in the Zhusileng tectonic zone (BGGP 1981a; BGNHAR

1982a). The lower part of Shuangbaotang Formation (previously the Maihanhada Formation) represents a normal neritic–coastal sedimentary environment and consists of clastic rocks and carbonates (BGMRIMAR 1991; Li et al. 1996). Its upper part (previously the Aqide Formation) comprises neritic clastic rocks and eruptive intermediate-acidic volcanic rocks in an oceanic basin (BGMRIMAR 1991; Li et al. 1996). In addition, the Upper Permian Haersuhai Formation is exposed in both the Huhetaoergai tectonic zone and the Zhusileng tectonic zone (BGGP 1980, 1981a; BGNHAR 1982a) and represents a flysch deposited in coastal, neritic and marine–terrestrial environments. It is in fault contact with the other strata (Wang et al. 1994). The lower part of the Haersuhai Formation comprises coarse clastic rocks, carbonates and intermediate-acidic volcanic rocks, and its upper part is composed of a thick section of fine clastic rocks and pelitic rocks with some limestone.

Sample descriptions

Wudenghan pluton

The Wudenghan pluton in the Zhusileng tectonic zone covers about 120 km^2 and was emplaced in the core of a late Carboniferous anticline (Fig. 3). Plutonic lithofacies are not well developed and consist mainly of biotite granodiorite and biotite monzogranite. As the whole pluton is highly weathered, especially the granodiorite, only the biotite monzogranite was studied. The monzogranite is medium-grained (3–5 mm). The modal mineralogy (Fig. 4a, b) includes plagioclase (25–35 %, mostly altered to sericite and partly altered to epidote), perthitic feldspar (25–40 %, partly altered to clay minerals), quartz (30–40 %), mafic minerals (8–15 %, mainly biotite, altered to chlorite) and minor muscovite. Zircon, monazite, apatite, hematite and magnetite are the main accessory minerals.

Huhetaoergai pluton

The Huhetaoergai pluton is in the Huhetaoergai tectonic zone and represents a batholith covering about 80 km^2. In the southeast, it intrudes Mesoproterozoic sandstone (Fig. 2). Banded structure and weakly developed gneissic fabric are present. The banded structure comprises 2- to 3-cm-wide light and dark parallel laminations. Generally, coarse quartz, plagioclase and feldspar comprise the light bands and fine biotite and plagioclase form the dark bands. Most minerals are aligned parallel to the bands. Elongate marble xenoliths parallel to the gneissic schistosity or laminations are also present (BGGP 1980).

The pluton is heterogeneous with variable composition and irregular lithofacies. However, it is predominantly fresh red biotite granite and gray biotite granodiorite. The biotite granite is the Neoproterozoic in age and intruded by the biotite granodiorite (Zhang et al. 2015). In this study, we mainly focus on the biotite granodiorite. It has a porphyritic-like texture. Most phenocrysts (8–24 mm) are euhedral–subhedral plagioclase (25–35 %). The matrix (<4 mm) includes plagioclase (35–45 %, partly altered to sericite and epidote), quartz (20–35 %, some recrystallization has occurred), biotite (15–20 %, partly altered to chlorite) and perthitic feldspar (10–15 %; Fig. 4c, d). Zircon, titanite, apatite, hematite and magnetite are the main accessory minerals.

Zhuxiaobuguhe pluton

The Zhuxiaobuguhe pluton is to the west of the Huhetao-ergai pluton in the Huhetaoergai tectonic zone (Fig. 2) and is larger than the Huhetaoergai pluton. Its northern part intrudes Middle Ordovician dacite and rhyolite. No clear evidence for recrystallization or thermal metamorphism is found in the wallrock, but the pluton has a well-developed foliation (Fig. 4e, f). Plutonic lithofacies are not well developed. Marble xenoliths have similar structures to those in the Huhetaoergai pluton (BGGP 1980).

The Zhuxiaobuguhe pluton consists mainly of porphyritic hornblende–biotite granodiorite (Fig. 4g, h). The phenocrysts (mostly 4–10 mm, some can reach 20 mm) include euhedral–subhedral plagioclase (10–30 %). The matrix (0.1–3 mm) includes plagioclase (40–50 %, mostly altered to sericite and epidote), quartz (15–25 %, with pronounced abundant recrystallization), hornblende (5–15 %, some altered to uralite and actinolite), biotite (10 %, mostly altered to chlorite) and perthitic feldspar (<5 %). Large subhedral titanite (about 1 mm) is abundant. Zircon, apatite, hematite and magnetite also occur as accessory minerals.

Analytical results

See "Analytical methods of electronic supplementary material" for a description of the analytical methods. For each pluton, 3–4 samples representing the batholiths' principal compositional phases were selected for major and trace element analyses. The results are given in "Table S1 of electronic supplementary material". After geochemical analyses, a representative sample of each pluton was selected for geochronology. One sample (AB10-48) was dated by LA-ICP-MS and two samples (W08-170 and AB10-30) by secondary ion mass spectrometry (SIMS). Analytical results are shown in "Tables S2 and S3 of electronic supplementary material", respectively. Integrating crystal shapes, textures and high Th/U ratios of the zircons, the majority of grains are presumed to be magmatic (Belousova et al. 2002;
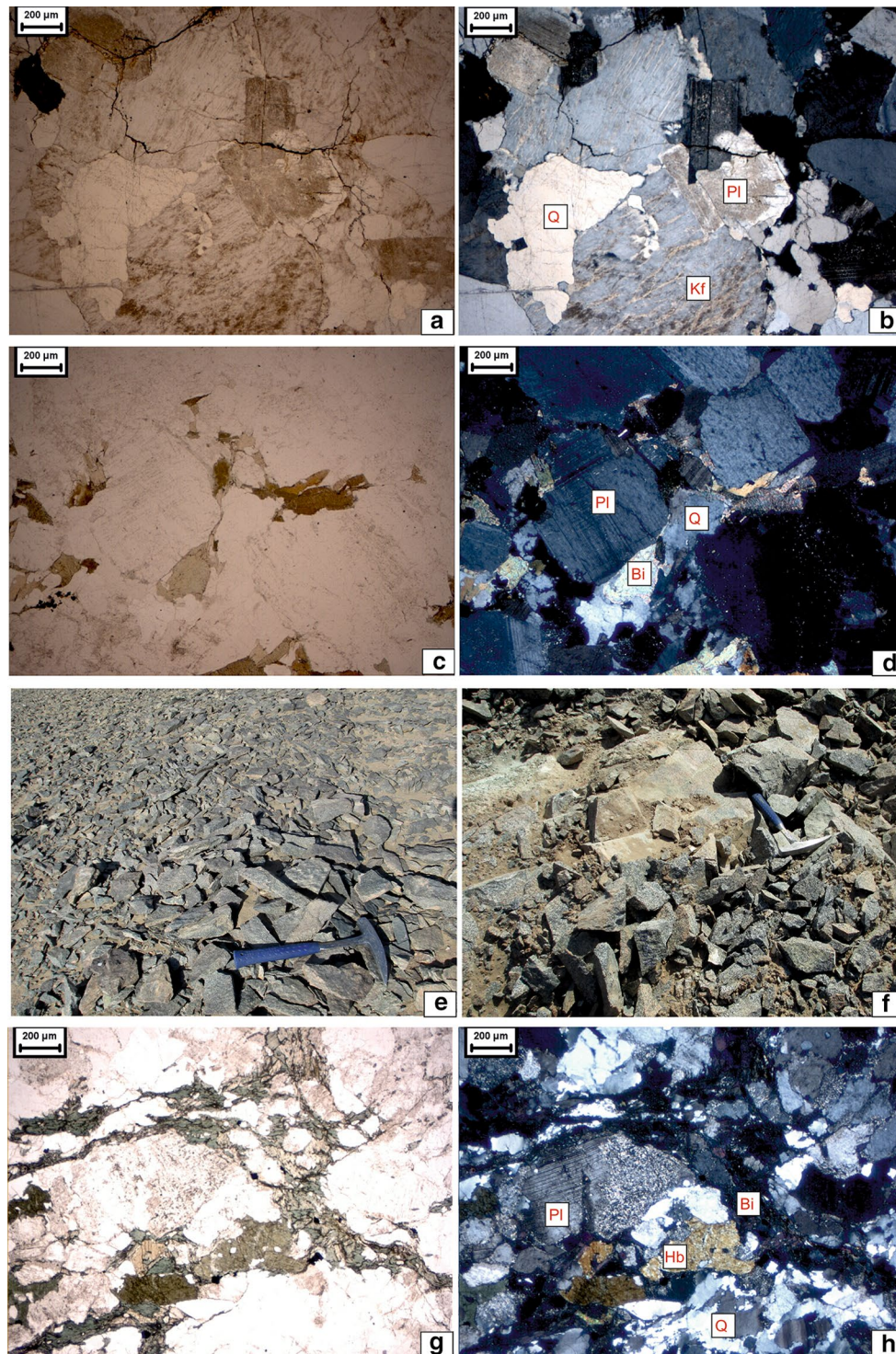
Fig. 4 Field photographs and microphotographs of late Paleozoic granites in the northernmost Alxa region. **a**, **b** Mineralogy of the Wudenghan monzogranite, *left* plane light, *right* cross-polars; **c**, **d**

Mineralogy of the Huhetaoergai granodiorite, *left* plane light, *right* cross-polars; **e**, **f** Zhuxiaobuguhe granodiorite; **g**, **h** Mineralogy of the Zhuxiaobuguhe granodiorite, *left* plane light, *right* cross-polars

Corfu et al. 2003). A few analyses showing apparently old (AB10-48-31, n4158-02 and 04) or discordant (n4159-08) ages, analyses on cracks (n4159-05 and 15) or inclusions

(n4159-14), or partly off the crystal (n4158-13, n4159-02, 03, 04 and 10), are excluded from the age calculations. The isotopic results are summarized in "Table S4 of electronic

supplementary material". Determination of "initial" conditions is based on the geochronology. Nd model ages have been calculated with $f_{Sm/Nd}$ of -0.2 to -0.6.

Wudenghan pluton

Major and trace elements

Wudenghan biotite monzogranite has high SiO_2 contents (>75 wt%) and low Al_2O_3 (12.27–13.09 wt%), CaO (0.44–0.67 wt%) and MgO (0.09–0.21 wt%) with low Mg# [0.14–0.27; $Mg^{2+}/(Mg^{2+} + Fe^{2+})$, Irving and Green 1976]. All samples are metaluminous (A/NCK < 1.1; Fig. 5a) and ferroan [Fe# = $FeO^T/(FeO^T + MgO)$ = 0.88–0.94] (after Frost et al. 2001). The total alkali content ($Na_2O + K_2O$) is 8.23 wt% on average, and all samples contain more K_2O than Na_2O (Na_2O/K_2O = 0.71–0.78). Using the classification of Irvine and Baragar (1971), the Wudenghan monzogranite represents the high-K calc-alkaline series (Fig. 5b). Chondrite-normalized REE patterns (Fig. 6a) show enrichment of LREE [$(La/Yb)_N$ = 4.5–6.3] and strongly negative Eu anomalies (δEu = 0.27–0.31). N-MORB-normalized trace element patterns (Fig. 6b) are enriched in LREE, Rb, U and K and depleted in Ba, Nb, Ti and Zr.

Geochronology

Zircon grains from this granite (AB10-30) are euhedral, clear to pink and transparent with aspect ratios (AR) of 1:1–3:1. Some grains have inclusions. In CL images, most show oscillatory or broad zoning (Fig. 7a). One core was found (n4159-03). Th/U ratios = 0.38–0.59. Seven analyses were concordant and combined to yield a concordia age of 383 ± 3 Ma (MSWD = 2.3; Fig. 8a), which is interpreted as the crystallization age for sample AB10-30.

Nd and Sr isotopes

The Wudenghan monzogranite has low initial $^{87}Sr/^{86}Sr$ of 0.704719–0.706113 and slightly negative $\varepsilon_{Nd}(t)$ of -0.2 to -0.1. They indicate Neoproterozoic-age components when intrusive age is plotted against $\varepsilon_{Nd}(t)$ (Fig. 9a). Single-stage model ages (T_{DM1}) are 1097–1123 Ma.

Huhetaoergai pluton

Major and trace elements

The Huhetaoergai biotite granodiorite has relatively lower SiO_2 (64.42–71.37 wt%) and TiO_2 (0.43–0.67 wt%) but much higher Al_2O_3 (14.88–17.95 wt%), CaO (2.87–4.20 wt%) and MgO (1.24–1.78 wt%) with high Mg# (0.49–0.53). Na_2O/K_2O ratios for the granodiorite are 1.9 on

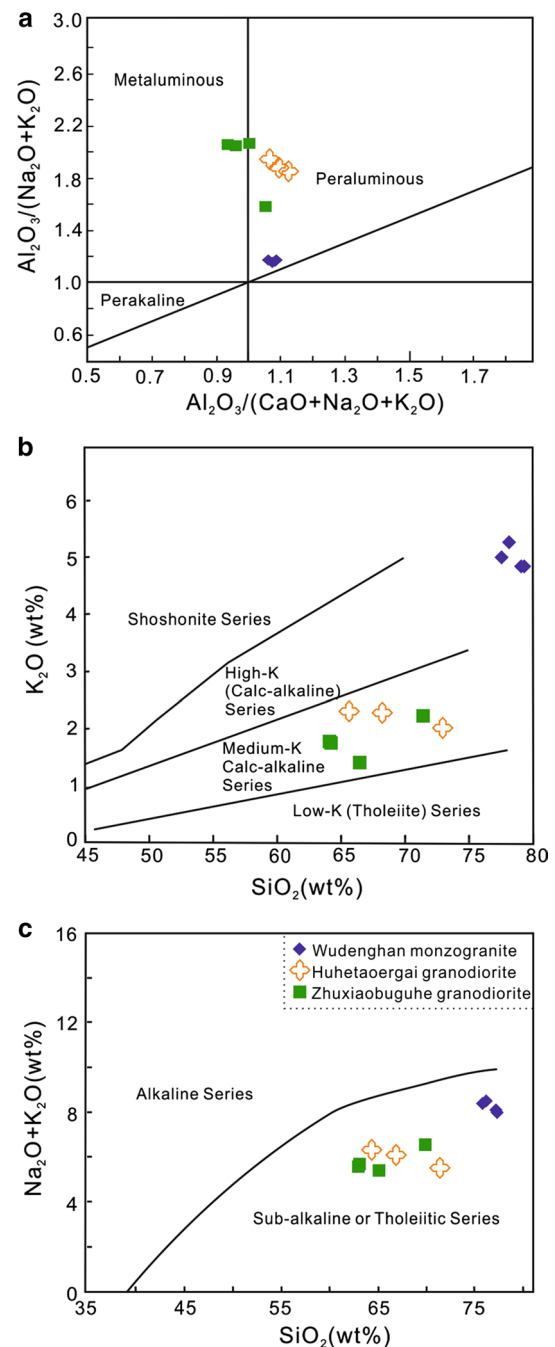**Fig. 5** Major element characteristics of the northernmost Alxa granites. **a** $Al_2O_3/(CaO + Na_2O + K_2O)$ versus $Al_2O_3/(Na_2O + K_2O)$ diagram (after Shand 1943); **b** SiO_2–K_2O diagram (fields from Rickwood 1989); **c** SiO_2 versus $Na_2O + K_2O$ diagram (after Irvine and Baragar 1971)

average with lower total alkali content (5.52–6.34 wt%) than the Huhetaoergai granodiorite. It is metaluminous to peraluminous (A/NCK = 1.07–1.12; Shand 1943; Zen 1988; Fig. 5a) and magnesian (Fe# = 0.69–0.71) and belongs to the medium-K calc-alkaline series (Fig. 5b, c). Chondrite-normalized REE patterns (Fig. 6c) show enrichment of
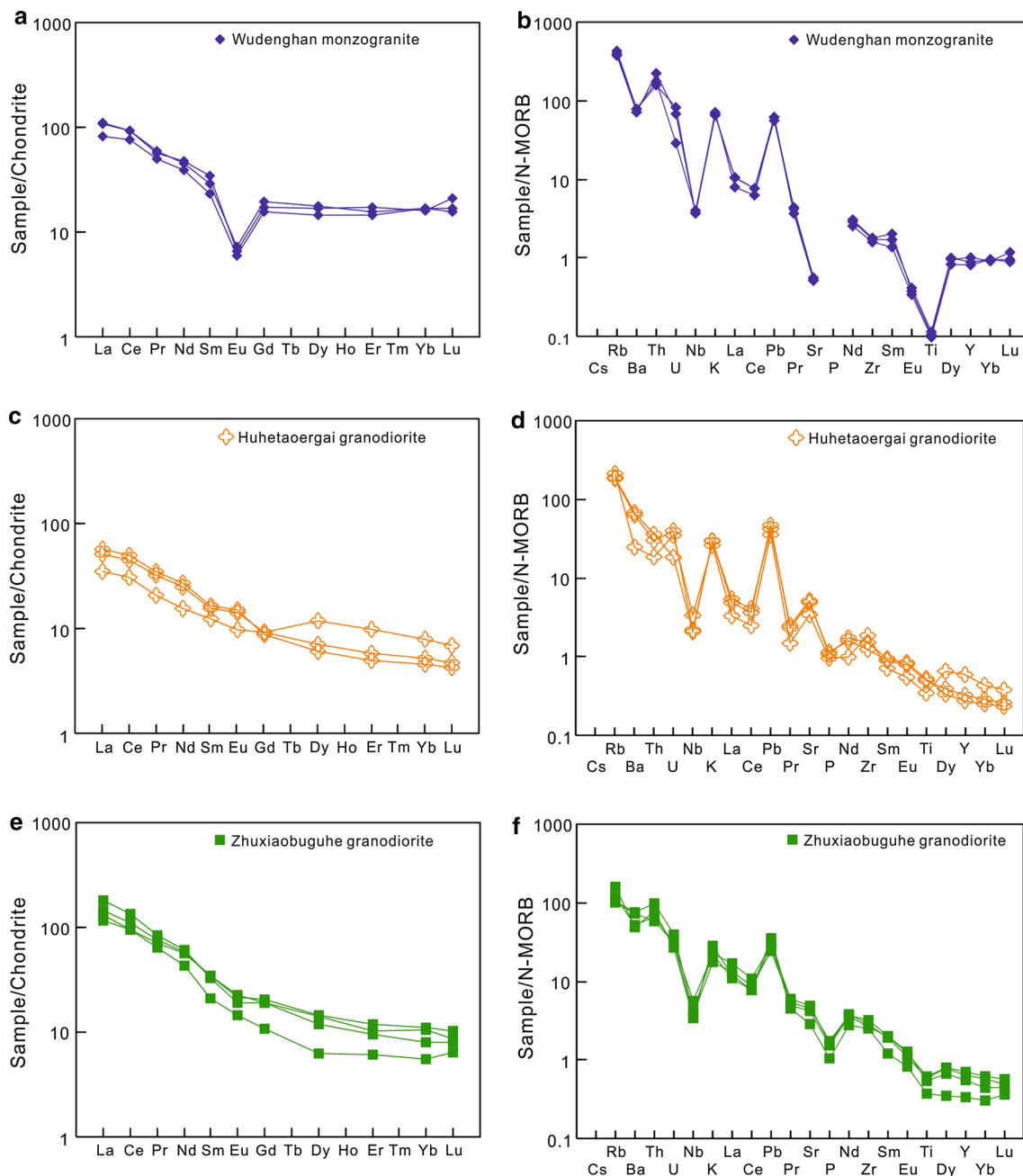
Fig. 6 Normalized REE and trace elements patterns for the Wudenghan (**a**, **b**), Huhetaoergai (**c**, **d**) and Zhuxiaobuguhe (**e**, **f**) samples. Chondrite and N-MORB normalization values from Sun and McDonough (1989)

LREE [(La/Yb)$_N$ = 4.2–11.9] and positive to slightly negative Eu anomalies (δEu = 0.91–1.25). N-MORB-normalized trace element patterns (Fig. 6d) show that the samples are enriched in Rb, K, Pb and Sr and depleted in Nb and P.

Geochronology

Zircon grains from this granite (AB10-48) are euhedral, clear to pink and transparent. AR ranges from 1:1 to 5:1.

Some have inclusions and inherited cores. Most analyses represent idiomorphic grains with oscillatory zoning throughout the crystal (Fig. 7b). Th/U = 0.09–3.45. One core was found and a slightly older age of 806 ± 22 Ma was obtained (AB10-48-31). Twenty-eight analyses combine to yield a concordia age of 356 ± 3 Ma (MSWD = 1.3; Fig. 8b), which is interpreted as the crystallization age for sample AB10-48.

Fig. 7 Cathodoluminescence (CL) images of zircons from the Wudenghan monzogranite (**a**), the Huhetaoergai pluton (**b**) and the Zhuxiaobuguhe granodiorite (**c**). All *scale bars* 50 μm

Zhuxiaobuguhe pluton

Major and trace elements

Major elements of the Zhuxiaobuguhe hornblende–biotite granodiorite have similar characteristics to the Huhetaoergai biotite granodiorite. SiO_2 contents range from 62.96 to 69.95 wt%, Al_2O_3 from 15.18 to 17.23 wt%, MgO from 1.29 to 2.31 wt% with high Mg# (0.49–0.53), TiO_2 (0.47–0.78 wt%) and CaO (2.66–5.46 wt%). All samples are metaluminous (A/NCK = 0.94–1.05; Fig. 5a) and magnesian (Fe# = 0.68–0.72). The total alkali content is between 5.37 and 6.54 wt%, and all samples contain more Na_2O than K_2O (Na_2O/K_2O = 2.11–3.13). Geochemically, the Zhuxiaobuguhe granodiorite represents a medium-K calc-alkaline pluton (Fig. 5b, c). Chondrite-normalized REE patterns (Fig. 6e) show higher enrichment of LREE [$(La/Yb)_N$ = 9.9–22.3] and weakly negative Eu anomalies (δEu = 0.77–0.96). N-MORB-normalized trace element patterns (Fig. 6f) show enrichments of LREE, Rb, K and Nd and depletions in Ba, Nb, Ti and P.

Geochronology

Zircon grains from this granite (W08-170) are euhedral, clear to pink and transparent with AR of 5:1. Some grains have inclusions. Most crystals have broad oscillatory zoning. Neither zircon cores nor old inherited ages

were obtained (Fig. 7c). The Th/U varies from 0.74 to 1.73. Eleven analyses combine to yield a concordia age of 286 ± 2 Ma (MSWD = 0.95; Fig. 8c), which is interpreted as the crystallization age for sample W08-170.

Nd and Sr isotopes

The Zhuxiaobuguhe granodiorite has initial $^{87}Sr/^{86}Sr$ of 0.708370–0.708462 and negative $\varepsilon_{Nd}(t)$ of −2.0 to −1.1 (Table S4). They indicate Neoproterozoic-age component with T_{DM1} = 1000–1013 Ma (Fig. 9a).

Discussion

Genesis of Late Paleozoic granites in the northernmost Alxa region

Late Devonian Wudenghan pluton

This pluton was previously considered to be Late Paleozoic in age (BGGP 1981a). Our new SIMS zircon U–Pb age from the biotite monzogranite (AB10-30) is 383 ± 3 Ma. From its mineralogical and geochemical characteristics, such as the absence of alkaline minerals, high SiO_2 contents (>75 wt%) and K_2O (>4.5 wt%), low Na_2O/K_2O and Ga/Al ratios, low MgO (<0.3 wt%), the Wudenghan monzogranite is interpreted to represent a highly fractionated

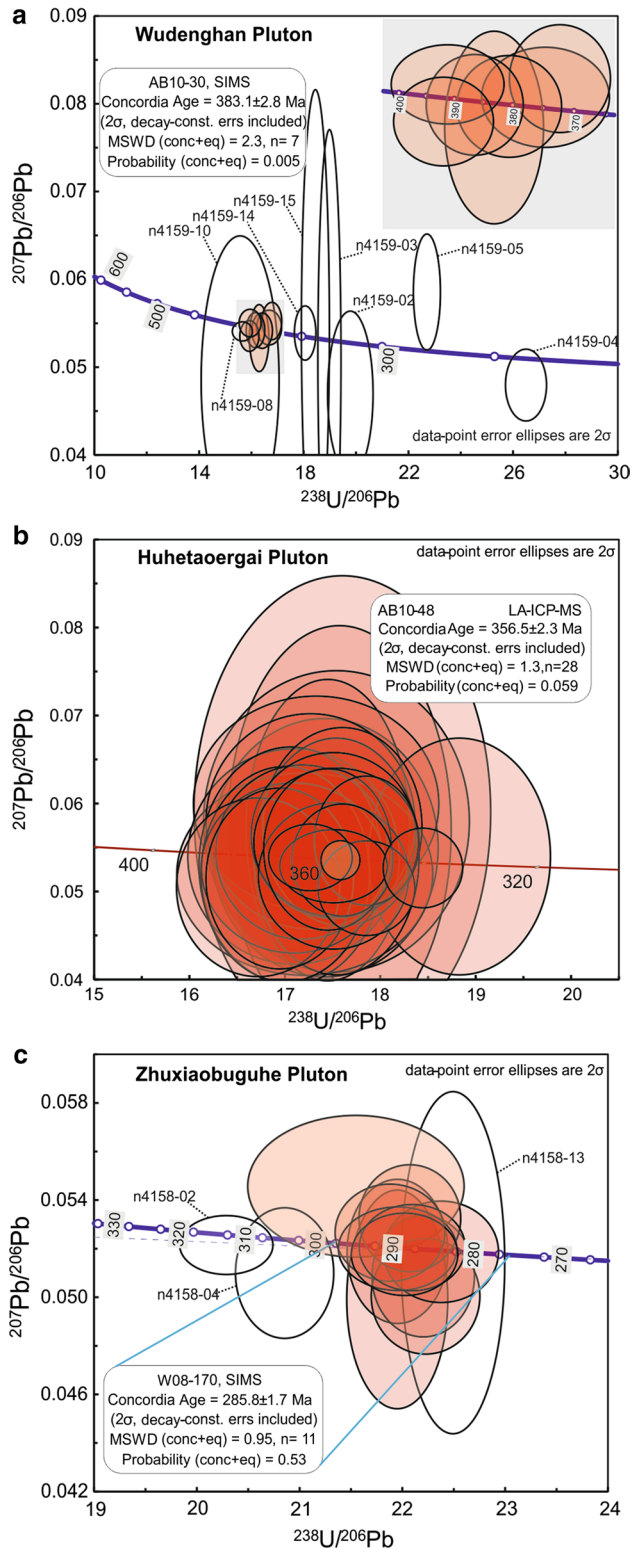**Fig. 8** U–Pb concordia plot for the Wudenghan monzogranite (**a**), the Huhetaoerguhi granodiorite (**b**) and the Zhuxiaobuguhe granodiorite (**c**). *Unfilled symbols* excluded from final synthesis. Plots generated using Isoplot (Ludwig 2003)
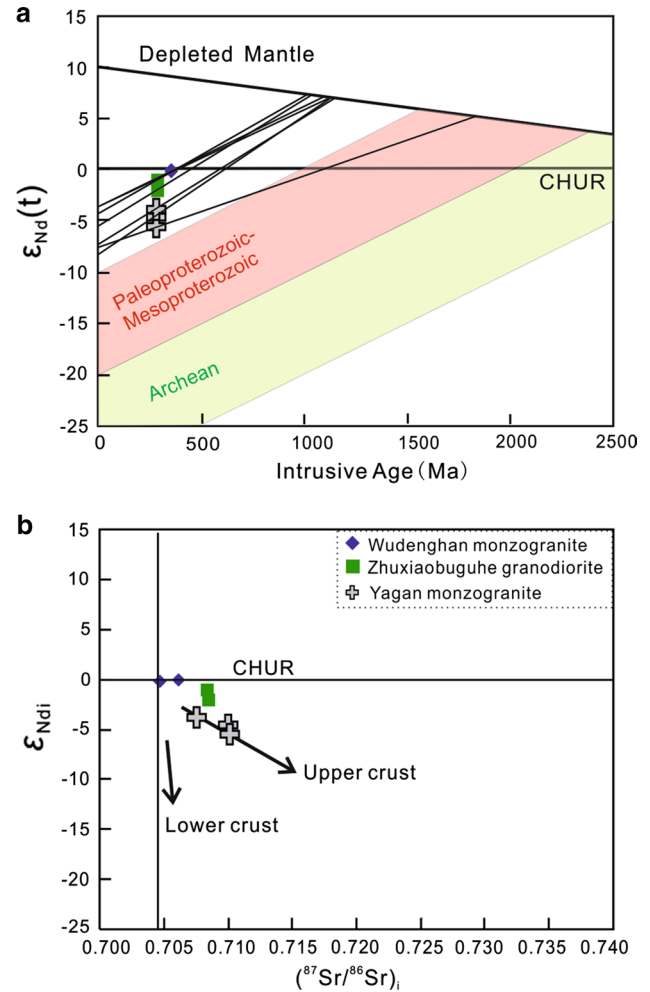

Fig. 9 Isotopic data. **a** $\varepsilon_{Nd}(t)$ versus intrusive age; **b** $\varepsilon_{Nd}(t)$ versus $(^{87}Sr/^{86}Sr)_i$ ratios [*lower* crust and *upper* crust fields from Wu et al. (2003)]

high-K calc-alkaline rock (e.g., Sylvester 1989; Whalen et al. 1987). It is metaluminous, with A/CNK < 1.1 and A/NK > 1, suggesting that it represents an I-type or A-type granitoid rather than S-type (Chappell and White 1992). The low Fe/Mg, Ga/Al and concentrations of Zr, Nb, Ga, Y, Ce, Sr and CaO further indicate that it is not an alkaline (A-type) granite but rather a fractionated felsic granite (Whalen et al. 1987). This is also supported by the striking depletions in Ba, Nb, Eu and Ti (Fig. 6b). Negative Nb–Ti anomalies are interpreted to relate to fractionation of Ti-bearing phases (ilmenite, titanite, rutile, etc.), negative P anomalies to result from apatite separation with strongly negative Eu anomalies requiring extensive fractionation of plagioclase and/or K-feldspar. The fractionation of K-feldspar would produce negative Eu–Ba anomalies. Therefore, the Wudenghan granite can be described as an evolved

I-type granite, possibly representing a fractionated melt(s) derived from a parental calc-alkaline magma.

Calc-alkaline, I-type granitoids are usually generated by (I) partial melting of mafic to intermediate igneous sources, (II) advanced assimilation and fractional crystallization of mantle-derived basaltic parental magmas, or (III) mixing of mantle-derived magmas with crustal-derived materials (e.g., De Paolo 1981; Li et al. 2007; Sisson et al. 2005; Hildreth and Moorbath 1988). Highly fractionated I-type granitoids can be formed by mixing of mantle wedge basaltic melts with associated induced crustal melts (Zhu et al. 2009). Plutons formed via mixing of different proportions between these two distinctive chemical and isotopic end-member compositions can only generate the relatively narrow isotopic and chemical composition of the Wudenghan pluton from homogeneous mixing and emplacement in a single melt batch. Based on the criteria employed by Watson and Harrison (1983), the zircon saturation temperature (T_{Zr}) calculated for the Wudenghan pluton yields values of 766–779 °C (average 772 °C). This pluton lacks inherited zircon, reflecting zircon-undersaturated melt compositions. Thus, T_{Zr} represents a minimum estimate of magma temperature (Miller et al. 2003). The low initial Sr isotopic ratios (0.704719–0.706113) combined with only slightly negative $\varepsilon_{Nd}(t)$ values (−0.2 to −0.1) for the Wudenghan pluton indicate a predominantly juvenile crustal source and only a minor older crustal component(s). Therefore, the Wudenghan pluton seems more likely to be generated from mantle-derived basaltic parental magmas with assimilation and fractional crystallization.

Early Carboniferous Huhetaoergai pluton

This pluton was previously considered to be early Paleozoic (BGGP 1980) or late Neoproterozoic in age (689 Ma, TIMS zircon U–Pb; Wang et al. 1994). Our new LA-ICP-MS zircon U–Pb age (AB10-48) is 356 ± 3 Ma. It represents the age of the Huhetaoergai biotite granodiorite pluton and resolves this controversy.

The high Na_2O/K_2O ratio and high Mg# (0.51 on average) indicate that the Huhetaoergai granodiorite represents an unfractionated calc-alkaline magma (Whalen et al. 1987). Smaller geochemical anomalies (Fig. 6) also suggest that fractionation was not extensive. Separation of feldspar from the Huhetaoergai granodiorite magma appears minor, as indicated by positive to slightly negative Eu anomalies. Positive Rb and Pb anomalies indicate the addition of a continental crustal component. The slightly high Mg# is consistent with input of primary mantle-derived melt (Kelemen et al. 1995). The zircon saturation temperature (T_{Zr}) calculated for the Huhetaoergai pluton is 737–779 °C (average 754 °C); the pluton has inherited zircons, indicating zirconium saturation, and therefore, the

T_{Zr} is considered to be a maximum initial magma temperatures at the source (Miller et al. 2003). According to Miller et al. (2003), the Huhetaoergai pluton represents a "cold" granite (T_{Zr} < 800 °C) which appears to form at temperatures too low for dehydration melting involving biotite or hornblende and probably requires fluid influx. Experiments and modeling indicate a water-rich fluid phase appears to be the only mechanism for inducing large-scale melting at T < 800 °C (Chappell et al. 2004; Miller et al. 2003). As early Carboniferous mafic rocks have not been recognized in the Huhetaoergai area before now, the suggestion of water-rich fluid in its source is enigmatic.

Early Permian Zhuxiaobuguhe pluton

The Zhuxiaobuguhe and Huhetaoergai plutons were previously regarded as a single pluton separated by Upper Jurassic and Quaternary strata (BGGP 1980; Wang et al. 1994). SIMS zircon U–Pb dating of the Zhuxiaobuguhe pluton (W08-170), however, gives an age of 286 ± 2 Ma. As no significant compositional diversity occurs in the Zhuxiaobuguhe pluton, we interpret this age to represent the age of the entire Zhuxiaobuguhe pluton. Therefore, the Zhuxiaobuguhe pluton was emplaced at 286 ± 2 Ma and is not contiguous with the Huhetaoergai pluton.

Similar to the Huhetaoergai granodiorite, the Zhuxiaobuguhe granodiorite represents unfractionated calc-alkaline melt (Whalen et al. 1987). Slightly negative initial ε_{Nd} (−2.0 to −1.1) and moderate initial $^{87}Sr/^{86}Sr$ (0.708370–0.708462) indicate of probably the crust–mantle interactions. The arc-like geochemical signature, such as enriched LREE coupled with negative Nb–Ta–Ti anomalies, is easily explained if inherited from the paleo-volcanic arc in the Huhetaoergai tectonic zone. Therefore, the Zhuxiaobuguhe pluton is most likely derived from partial melting of mafic to intermediate igneous arc sources.

It is notable that the Yagan pluton of similar age (283 ± 2 Ma, SIMS zircon U–Pb) also occurs in the Huhetaoergai tectonic zone (Fig. 3; Zheng et al. 2013). The Yagan monzogranite represents unfractionated metaluminous to peraluminous high-K calc-alkaline granodiorite melt. It has higher SiO_2 (66.96–70.71 wt%) and total alkali contents ($Na_2O + K_2O$ = 7.24–9.19 wt%), with lower TiO_2 (0.21–0.29 wt%), CaO (2.07–2.43 wt%) and Na_2O/K_2O (1.04–1.34). The chondrite-normalized REE patterns show less enrichment of LREE [$(La/Yb)_N$ = 5.0–11.0] and more negative Eu anomalies (δEu = 0.59–0.77). Compared with the Zhuxiaobuguhe granodiorite, the Yagan monzogranite has lower initial $\varepsilon_{Nd}(t)$, similar initial $^{87}Sr/^{86}Sr$ (Fig. 9b; Table 1) and an older T_{DM1} age (1162–1821 Ma; Zheng et al. 2013). Consistent with the Zhuxiaobuguhe pluton, the T_{Zr} of the Yagan pluton is also lower than 800 °C (743–768 °C, average 754 °C) with inherited zircon. Therefore,

Table 1 Summary of northernmost Alxa granitic plutons

Pluton	Latitude and longitude	Zone	U–Pb age (Ma)	Chemical signature					Tectonic setting	References
				Isotopes		Traces				
				$\varepsilon_{Nd}(t)$	$(^{87}Sr/^{86}Sr)_I$	$(La/Yb)_N$	δEu	Other		
Wudenghan pluton	41°48′27″N 102°46′34″E	ZZ	383 ± 3	−0.2	0.705416	4.5–6.3	0.27–0.31	Enriched in Rb, K and U Depleted in Ba, Nb, Ti, P and Zr	Volcanic arc (related to the northward subduction of the oceanic basin represented by the Engger Us ophiolitic belt)	This study
Huhetaoergai pluton	42°00′56″N 101°39′27″E	HZ	356 ± 3			4.2–11.9	0.91–1.25	Enriched in Rb, K, Pb and Sr Depleted in Nb and P	Volcanic arc (related to the northward subduction of the oceanic basin represented by the Yagan Suture)	This study
Zhuxiaobuguhe pluton	42°01′02″N, 101°31′45″E	HZ	286 ± 2	−1.6	0.708416	9.9–22.3	0.77–0.96	Enriched in Rb, Th, K and Nd Depleted in Ba, Nb, Ti and P	Extensional (after all oceanic basins closed, the northernmost Alxa region underwent extension)	This study
Yagan pluton	42°05′45″N, 101°30′09″E	HZ	283 ± 2	−4.6	0.709334	5.0–11.0	0.59–0.77	Enriched in Rb, K, Th, Nd and Sr Depleted in Ba, Nb, Ti, P and Zr	Extensional (after all oceanic basins closed, the northernmost Alxa region underwent extension)	Zheng et al. (2013)

HZ Huhetaoergai tectonic zone, *ZZ* Zhusileng tectonic zone

we suggest that early Permian granites in the Huhetaoergai tectonic zone were generated from partial melting of mafic lower crust of the paleo-volcanic arc.

Tectonic implications

Wudenghan pluton

All samples from the Wudenghan monzogranite have highly fractionated calc-alkaline, volcanic arc and post-collisional characteristics (Pearce 1996; Whalen et al. 1987). Almost all highly fractionated granites converge in major and trace element geochemistry to resemble each other, no matter which tectonic environment they form in. It is very difficult to use highly fractionated melts to infer tectonic environments. Furthermore, arc-like geochemical signatures, such as enriched LREE coupled with negative Nb–Ta–Ti anomalies, can be inherited from any source with subduction zone chemistry.

An additional complication from the sedimentary record inhibits understanding whether the late Devonian Wudenghan pluton represents a post-collisional granite or volcanic arc granite and hinges on the interpretation of the Wotuoshan Formation in the Zhusileng tectonic zone. The Wudenghan pluton intrudes the Zhusileng tectonic zone (Figs. 1c, 3) which represents a passive continental margin from Cambrian to Middle Silurian time (Wang et al. 1994; Wu et al. 1998). On the one hand, Wang et al. (1994) thought the ocean between the Zhusileng tectonic zone and Huhetaoergai tectonic zone closed during late Silurian–Devonian time because the Middle Devonian Wotuoshan Formation in the Zhusileng tectonic zone represented a marine molasse. However, it is highly debated whether the Wotuoshan Formation actually represents a molasses: The lower part of the Wotuoshan Formation is composed of conglomerate and pebbly coarse sandstone, the middle part includes varicolored calcic feldspathic quartz sandstone, calcic tuffaceous sandstone and siltstone with thin-layered limestone, and the upper part includes medium-coarse feldspathic quartz sandstone. On the other hand, Wu et al. (1998) suggested that Devonian deposition in the Zhusileng tectonic zone implied a stable littoral environment and that during the Carboniferous the Zhusileng tectonic zone changed from a passive to an active margin associated with the northward subduction of the oceanic crust represented by the Engger Us ophiolitic belt.

Whether the late Devonian Wudenghan pluton represents a post-collisional granite or volcanic arc granite is crucial for constraining the tectonic environment of Devonian Zhusileng tectonic zone. If the Wudenghan pluton formed in post-collisional setting, it is difficult to explain the source of relatively juvenile mantle input

[indicated by higher $\varepsilon_{Nd}(t)$ (−0.2 to −0.1) and very low $({}^{87}Sr/{}^{86}Sr)_t = 0.704719$–0.706113]. As the early Carboniferous Huhetaoergai pluton also formed in a volcanic arc environment (see "Huhetaoergai pluton" section) and the oceanic crust represented by the Yagan Suture did not seem to subduct southward during Devonian time, we suggest that the late Devonian Wudenghan pluton formed by the northward subduction of the oceanic crust represented by the Engger Us ophiolitic belt. This is also supported by the early–middle Paleozoic rock distributions in the Northern Alxa region (Fig. 1c), which probably indicate southeastward younging and migration of arc magmatism from Ordovician to Devonian time. Therefore, the Wudenghan pluton is more likely to have formed during subduction–accretion processes rather than in a post-collisional setting. It provides new evidence that the basin between the Zhusileng tectonic zone and Huhetaoergai tectonic zone was not closed before Late Devonian time (Fig. 10).
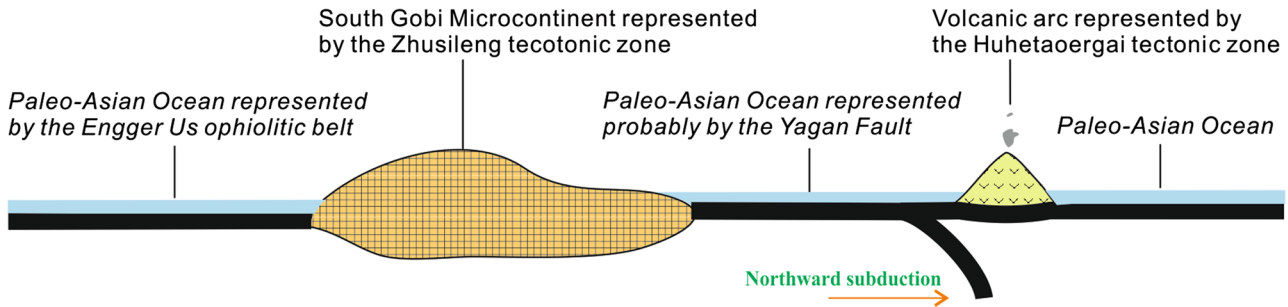
Huhetaoergai pluton

The early Carboniferous Huhetaoergai granodiorite has trace element compositions associated with a volcanic arc granite (Pearce 1996; Pearce et al. 1984). This is consistent with the sedimentary record in the Huhetaoergai tectonic zone (BGGP 1980) which also reflects a volcanic arc environment during the early Carboniferous. The Lower Carboniferous strata with continuous deposition of acidic volcanic rocks in the lower part and clastic rocks in the upper part represent a littoral-neritic depositional setting. It is only exposed in the extreme north near Mongolia. The lower part of Upper Carboniferous strata, in contact with Lower Carboniferous strata by a fault, also represents a littoral environment. From bottom to top, they include fine-grained arkosic graywacke interbedded with intermediate volcanic rocks, intermediate-acidic volcanic rocks and quartz sandstone. The fault contact is exposed between the bottom and middle layers. In addition, the uppermost Upper Carboniferous strata have not been recognized in the Huhetaoergai tectonic zone until now. The geochemistry of the Huhetaoergai granodiorite combined with the sedimentary history of the region indicates that the Huhetaoergai area is likely to represent a volcanic arc setting during early Carboniferous time, and the oceanic basin was still open at that time (Fig. 10). This is also supported by studies of the linked Mongolia terranes. The Huhetaoergai tectonic zone extends to the northeast into Mongolia as the Hashaat Terrane, which is interpreted as fragments of island arcs of the Paleo-Asian Ocean system (Badarch et al. 2002 and references therein). It occurs between the back-arc basin represented by the Atasbogad Terrane and the cratonal block represented by the Tsagaan Uul Terrane of southern Mongolia.
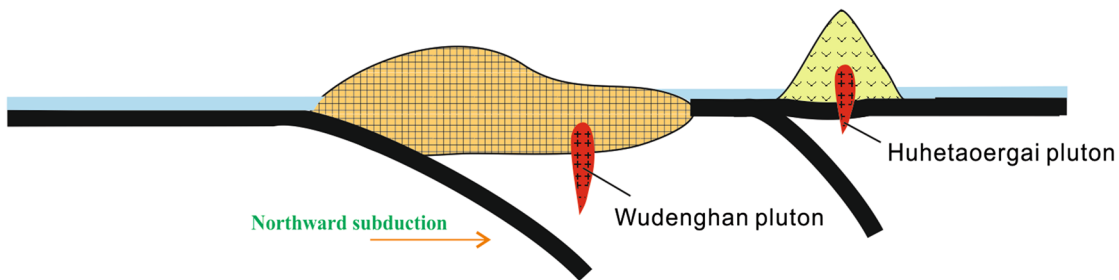
a Middle Ordovician - Middle Silurian

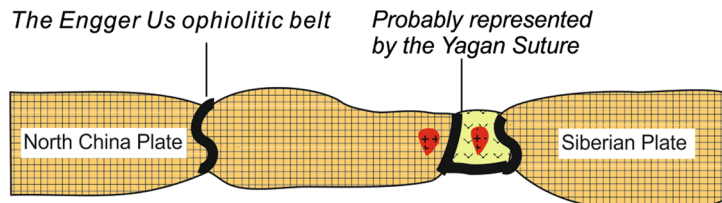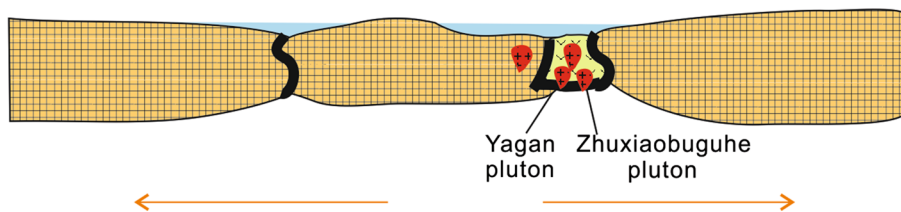S   N

South Gobi Microcontinent represented
by the Zhusileng tecotonic zone

Volcanic arc represented by
the Huhetaoergai tectonic zone

*Paleo-Asian Ocean represented
by the Engger Us ophiolitic belt*

*Paleo-Asian Ocean represented
probably by the Yagan Fault*

Paleo-Asian Ocean

Northward subduction

b Late Silurian - Early Carboniferous

Huhetaoergai pluton

Northward subduction

Wudenghan pluton

c Late Carboniferous

The Engger Us ophiolitic belt

*Probably represented
by the Yagan Suture*

North China Plate

Siberian Plate

d Early Permian

Legend

Continental Crust

Oceanic Crust

Volcanic arc

Granite

Oceanic water

Yagan
pluton

Zhuxiaobuguhe
pluton

Fig. 10 a–f Schematic tectonic evolution of the northernmost Alxa region. See text for details. Based on data from this study, Wang et al. (1994), Wu et al. (1998), Zhang et al. (2013a) and Zheng et al. (2013)

The Jindouaobao gneiss (Wang et al. 2001) testifies that the Zhusileng tectonic zone is the continuation of the Tsagaan Uul Terrane, and they may represent a part of the South Gobi microcontinent (Badarch et al. 2002). Lamb and Badarch (2001) pointed out that the Devonian strata of southern Mongolia represented components of two arc systems, including a trapped ocean basin that developed into a back-arc basin (e.g., the Atasbogad Terrane, Badarch et al. 2002). The Carboniferous arc was probably a continuation of the Devonian arc system and was built in part upon Devonian strata (e.g., the Hashaat Terrane, Badarch et al. 2002). Consistent with studies in southern Mongolia, the early Carboniferous Huhetaoergai tectonic zone reflects a volcanic arc environment. Therefore, the Huhetaoergai pluton is interpreted to represent a volcanic arc granite.

Zhuxiaobuguhe pluton

Early Permian granitoids of the CAOB typically have post-collisional signatures (Glorie et al. 2011; Han et al. 1997, 1999; Heinhorst et al. 2000; Wang et al. 2009). Trace element compositions of samples from the Zhuxiaobuguhe pluton are consistent with volcanic arc to post-collisional settings (Pearce 1996; Pearce et al. 1984). Samples from Yagan monzogranite of similar age (283 ± 2 Ma) in the Huhetaoergai tectonic zone are also reported to have both volcanic arc and post-collisional characteristics (Zheng et al. 2013; Fig. 3). Previously, two distinct tectonic environments have been suggested for the Huhetaoergai tectonic zone in the Permian (Wang et al. 1994; Wu et al. 1998). Wu et al. (1998) argued northward subduction of oceanic crust between the Huhetaoergai tectonic zone and the Zhusileng tectonic zone in the Permian resulted in rifting of the Zhusileng tectonic zone. However, though Wang et al. (1994) agreed that in the Permian the Zhusileng tectonic zone was in a rifting stage, they suggested that this was the result of the southward subduction of oceanic crust represented by the Engger Us Ophiolitic Belt and that the Permian Huhetaoergai–Zhusileng tectonic zones together were involved in rifting. Sedimentary investigations show the Permian strata of the Huhetaoergai tectonic zone and Zhusileng tectonic zone may be correlated (BGGP 1980, 1981a; Wang et al. 1994; Wu et al. 1998). In this case, there would not be an ocean between Huhetaoergai tectonic zone and Zhusileng tectonic zone in the Permian. Lamb and Badarch (2001) pointed out that Permian strata record mainly nonmarine basins, as well as the closing of the ocean basin between southern Mongolia and the tectonic blocks of China. Consequently, we conclude that the Permian Huhetaoergai tectonic zone represents a rifting environment rather than an active margin (Fig. 10d).

Tectonic model

To summarize, this study combined with previous investigations into granite genesis (Zheng et al. 2013; Table 1) and the tectonic evolution of the region (Wang et al. 1994; Wu et al. 1998) allows us to develop a new late Paleozoic tectonic scenario for the evolution of the northernmost Alxa region (Fig. 10).

- Middle Ordovician–Middle Silurian (Fig. 10a): The Paleo-Asian Ocean (now represented probably by the Yagan Suture) started to subduct northward from at least the Middle Ordovician and the volcanic arc represented by the Huhetaoergai tectonic zone formed in the oceanic basin. The Zhusileng tectonic zone represents a passive continental margin (Wang et al. 1994).
- Late Silurian–early Carboniferous (Fig. 10b): The oceanic basin between the Huhetaoergai tectonic zone and Zhusileng tectonic zone continued subducting northward. In the early Carboniferous, the Western Huhetaoergai granodiorite formed in a volcanic arc. Meanwhile, in the south, the oceanic crust represented by the Engger Us Ophiolitic Belt began subducting northward and resulted in the Late Devonian highly fractionated I-type Wudenghan granite.
- Late Carboniferous (Fig. 10c): The ocean between the Huhetaoergai tectonic zone and Zhusileng tectonic zone closed in the northern Alxa region and the Yagan Suture formed.
- Early Permian (Fig. 10d): The Huhetaoergai–Zhusileng tectonic zones entered into a period of extension allowing the Zhuxiaobuguhe and Yagan plutons to be emplaced.

Conclusions

1. The late Devonian Wudenghan monzogranite is a highly fractionated calc-alkaline granite with higher initial ε_{Nd} (-0.2 to -0.1) and low initial $^{87}Sr/^{86}Sr$ values (0.704719–0.706113). It probably represents a highly fractionated volcanic arc granite formed in response to the northward subduction of the oceanic basin represented by the Engger Us ophiolitic belt.
2. Early Carboniferous Huhetaoergai granodiorite formed in a volcanic arc setting. It formed mainly by the partial melting of lower continental crust. During the early Carboniferous, the oceanic basin between the Huhetaoergai tectonic zone and the Zhusileng tectonic zone still existed.
3. The early Permian Zhuxiaobuguhe pluton is not part of the Huhetaoergai pluton. It is composed of unfrac-

tionated calc-alkaline granodiorite with low initial ε_{Nd} (-2.0 to -1.1) and moderate initial $^{87}Sr/^{86}Sr$ values (0.708370–0.708462). The magma is derived from partial melting of mafic lower crust of the paleo-volcanic arc. The Huhetaoergai tectonic zone entered into the post-collisional extensional stage during early Permian.

References

Badarch G, Dickson Cunningham W, Windley BF (2002) A new terrane subdivision for Mongolia: implications for the Phanerozoic crustal growth of Central Asia. J Asian Earth Sci 21:87–110

Belousova EA, Griffin WL, O'Reilly SY, Fisher NI (2002) Igneous zircon: trace element composition as an indicator of source rock type. Contrib Mineral Petrol 143:602–622

BGGP (Bureau of Geology, Gansu Province) (1979) Guaizihunan and Yingejing Sheets Regional Geological Survey Report (1:200000) (in Chinese)

BGGP (Bureau of Geology, Gansu Province) (1980) Suoguonao Sheet Regional Geological Survey Report (1:200000) (in Chinese)

BGGP (Bureau of Geology, Gansu Province) (1981a) Yagan and Guaizihu Sheets Regional Geological Survey Report (1:200000) (in Chinese)

BGGP (Bureau of Geology, Gansu Province) (1981b) Jianguoying, Ejinaqi, Huxixincun, Wutaohai, Xianshui and Gulunai Sheets Regional Geological Survey Report (1:200000) (in Chinese)

BGIMAR (Bureau of Geology, Inner Mongolia Autonomous Region) (1980) Wuerte and Hailisu Geological Survey Report (1:200000) (in Chinese)

BGMRIMAR (Bureau of Geology and Mineral Resources, Inner Mongolia Autonomous Region) (1991) Regional Geology of Inner Mongolia. Geological Publishing House, Beijing **(in Chinese)**

BGNHAR (Bureau of Geology, Ningxia Hui Autonomous Region) (1976) Qinggeletu Sheet Regional Geological Survey Report (1:200000) (in Chinese)

BGNHAR (Bureau of Geology, Ningxia Hui Autonomous Region) (1980a) Wuliji Sheet Regional Geological Survey Report (1:200000) (in Chinese)

BGNHAR (Bureau of Geology, Ningxia Hui Autonomous Region) (1980b) Yingen Sheet Regional Geological Survey Report (1:200000) (in Chinese)

BGNHAR (Bureau of Geology, Ningxia Hui Autonomous Region) (1980c) Kunaitoulamamiao Sheet Regional Geological Survey Report (1:200000) (in Chinese)

BGNHAR (Bureau of Geology, Ningxia Hui Autonomous Region) (1980d) Alatanaobao Sheet Regional Geological Survey Report (1:200000) (in Chinese)

BGNHAR (Bureau of Geology, Ningxia Hui Autonomous Region) (1982a) Hariaoribuerge Sheet Regional Geological Survey Report (1:200000) (in Chinese)

BGNHAR (Bureau of Geology, Ningxia Hui Autonomous Region) (1982b) Shalataoerhan Sheet Regional Geological Survey Report (1:200000) (in Chinese)

Chappell BW, White AJR (1992) I- and S-type granites in the Lachlan Fold Belt. Trans R Soc Edinb Earth Sci 83:1–26

Chappell BW, White AJR, Williams IS, Wyborn D (2004) Low- and high-temperature granites. Trans R Soc Edinb Earth Sci 95(Parts 1–2):125–140

Corfu F, Hanchar JM, Hoskin PWO, Kinny P (2003) Atlas of zircon textures. Rev Mineral Geochem 53:469–500

Dan W, Li X-H, Wang Q, Wang X-C, Liu Y (2014) Neoproterozoic S-type granites in the Alxa Block, westernmost North China and tectonic implications: in situ zircon U–Pb–Hf–O isotopic and geochemical constraints. Am J Sci 314:110–153

De Paolo DJ (1981) Trace element and isotopic effects of combined wallrock assimilation and fractional crystallization. Earth Planet Sci Lett 53:189–202

Feng J, Xiao W, Windley B, Han C, Wan B, Zhang Je, Ao S, Zhang Z, Lin L (2013) Field geology, geochronology and geochemistry of mafic–ultramafic rocks from Alxa, China: implications for Late Permian accretionary tectonics in the southern Altaids. J Asian Earth Sci 78:114–142

Frost BR, Barnes CG, Collins WJ, Arculus RJ, Ellis DJ, Frost CD (2001) A geochemical classification for granitic rocks. J Petrol 42:2033–2048

Geng Y, Zhou X (2012) Early Permian magmatic events in the Alxa metamorphic basement: evidence from geochronology. Acta Petrol Sin 28:2667–2685 **(in Chinese with English abstract)**

Geng Y, Wang X, Shen Q, Wu C (2002) The discovery of Neoproterozoic Jinningian deformed granites in Alax area and its significance. Acta Petrol Mineral 21:412–421 **(in Chinese with English abstract)**

Glorie S, De Grave J, Buslov MM, Zhimulev FI, Izmer A, Vandoorne W, Ryabinin A, Van den Haute P, Vanhaecke F, Elburg MA (2011) Formation and paleozoic evolution of the Gorny-Altai–Altai-Mongolia suture zone (South Siberia): zircon U/Pb constraints on the igneous record. Gondwana Res 20:465–484

Han BF, Wang SG, Jahn BM, Hong DW, Kagami H, Sun YL (1997) Depleted-mantle source for the Ulungur River A-type granites from North Xinjiang, China: geochemistry and Nd–Sr isotopic evidence, and implications for Phanerozoic crustal growth. Chem Geol 138:135–159

Han B, He G, Wang S (1999) Postcollisional mantle-derived magmatism, underplating and implications for basement of the Junggar Basin. Sci China Ser D Earth Sci 42:113–119

Heinhorst J, Lehmann B, Ermolov P, Serykh V, Zhurutin S (2000) Paleozoic crustal growth and metallogeny of Central Asia: evidence from magmatic-hydrothermal ore systems of Central Kazakhstan. Tectonophysics 328:69–87

Hildreth W, Moorbath S (1988) Crustal contributions to arc magmatism in the Andes of Central Chile. Contrib Mineral Petrol 98:455–489

Irvine TN, Baragar WRA (1971) A guide to the chemical classification of the common volcanic rocks. Can J Earth Sci 8:523–548

Irving AJ, Green DH (1976) Geochemistry and petrogenesis of the newer basalts of Victoria and South Australia. J Geol Soc Aust 23:45–66

Jahn BM, Wu FY, Chen B (2000) Granitoids of the Central Asian Orogenic Belt and continental growth in the Phanerozoic. Geol Soc Am Spec Pap 350:181–193

Kelemen PB, Shimizu N, Salters VM (1995) Extraction of mid-ocean-ridge basalt from the upwelling mantle by focused flow of melt in dunite channels. Nature 375:747–753

Kröner A, Alexeiev DV, Hegner E, Rojas-Agramonte Y, Corsini M, Chao Y, Wong J, Windley BF, Liu D, Tretyakov AA (2012) Zircon and muscovite ages, geochemistry, and Nd–Hf isotopes for the Aktyuz metamorphic terrane: evidence for an Early Ordovician collisional belt in the northern Tianshan of Kyrgyzstan. Gondwana Res 21:901–927

Kröner A, Kovach V, Belousova E, Hegner E, Armstrong R, Dolgopolova A, Seltmann R, Alexeiev D, Hoffmann J, Wong J (2014) Reassessment of continental growth during the accretionary history of the Central Asian Orogenic Belt. Gondwana Res 25:103–125

Lamb MA, Badarch G (2001) Paleozoic sedimentary basins and volcanic arc systems of southern Mongolia: new geochemical and petrographic constraints. In: Davis GA, Hendrix MS (eds) Paleozoic and mesozoic tectonic evolution of Central and Eastern Asia: from continental assembly to intracontinental deformation. Geol Soc Am, pp 117–149

Li W, Li Q, Jiang W (1996) Stratigraphy (Lithostratic) of Nei Mongol (Inner Mongolia) Autonomous Region. China University of Geosciences Press, Wuhan **(in Chinese)**

Li XH, Li ZX, Li WX, Liu Y, Yuan C, Wei G, Qi C (2007) U–Pb zircon, geochemical and Sr–Nd–Hf isotopic constraints on age and origin of Jurassic I- and A-type granites from central Guangdong, SE China: a major igneous event in response to foundering of a subducted flat-slab? Lithos 96:186–204

Ludwig KR (2003) Isoplot 3.0: a geochronological toolkit for microsoft excel. Berkeley Geochronology Center, Berkeley, Special Publication 4, pp 1–71

Miller CF, McDowell SM, Mapes RW (2003) Hot and cold granites: implications of zircon saturation temperatures and preservation of inheritance. Geology 31:529–532

Pearce JA (1996) Sources and settings of granitic rocks. Episodes 19:120–125

Pearce JA, Harris NBW, Tindle AG (1984) Trace-element discrimination diagrams for the tectonic interpretation of granitic-rocks. J Petrol 25:956–983

Ran H, Zhang WJ, Liu Z (2012) Geochemical characteristics and LA–ICP–MS zircon U–Pb dating of the Late Permian monzogranite in Hanggale, Alax Right Banner, Inner Mongolia. Geol Bull China 31:1565–1575 **(in Chinese with English abstract)**

Rickwood PC (1989) Boundary lines within petrologic diagrams which use oxides of major and minor elements. Lithos 22:247–263

Şengör AMC, Natal'In BA, Burtman VS (1993) Evolution of the Altaid tectonic collage and Palaeozoic crustal growth in Eurasia. Nature 364:299–307

Shand SJ (1943) Eruptive rocks: their genesis, composition, and classification, with a chapter on meteorites, 2nd edn. Wiley, New York

Shi X, Tong Y, Wang T, Zhang J, Zhang Z, Zhang L, Guo L, Zeng T, Geng J (2012) LA–ICP–MS zircon U–Pb age and geochemistry of the Early Permian Halinudeng granite in northern Alxa area, western Inner Mongolia. Geol Bull China 31:662–670 **(in Chinese with English abstract)**

Shi X, Wang T, Zhang L, Castro A, Xiao X, Tong Y, Zhang J, Guo L, Yang Q (2014) Timing, petrogenesis and tectonic setting of the Late Paleozoic gabbro–granodiorite–granite intrusions in the Shalazhashan of northern Alxa: constraints on the southernmost boundary of the Central Asian Orogenic Belt. Lithos 208:158–177

Sisson TW, Ratajeski K, Hankins WB, Glazner AF (2005) Voluminous granitic magmas from common basaltic sources. Contrib Mineral Petrol 148:635–661

Sun SS, McDonough WF (1989) Chemical and isotopic systematics of oceanic basalts: implications for mantle composition and processes. In: Saunders AD, Norry MJ (eds) Magmatism in the Ocean Basins. Geol Soc, Spec Publ 42, pp 313–345

Sylvester PJ (1989) Post-collisional alkaline granites. J Geol 97:261–280

Wang T, Wang S, Wang J (1994) The formation and evolution of paleozoic continental crust in Alax region. Lanzhou University Press, Lanzhou **(in Chinese with English abstract)**

Wang T, Zheng Y, Gehrels GE, Mu Z (2001) Geochronological evidence for existence of South Mongolian microcontinent—a zircon U–Pb age of grantoid gneisses from the Yagan-Onch Hayrhan metamorphic core complex. Chin Sci Bull 46:2005–2008

Wang T, Jahn BM, Kovach VP, Tong Y, Hong DW, Han BF (2009) Nd–Sr isotopic mapping of the Chinese Altai and implications for continental growth in the Central Asian Orogenic Belt. Lithos 110:359–372

Watson EB, Harrison TM (1983) Zircon saturation revisited: temperature and composition effects in a variety of crustal magma types. Earth Planet Sci Lett 64:295–304

Whalen JB, Currie KL, Chappell BW (1987) A-type granites: geochemical characteristics, discrimination and petrogenesis. Contrib Mineral Petrol 95:407–419

Wilhem C, Windley BF, Stampfli GM (2012) The Altaids of Central Asia: a tectonic and evolutionary innovative review. Earth-Sci Rev 113:303–341

Windley BF, Alexeiev D, Xiao WJ, Kroner A, Badarch G (2007) Tectonic models for accretion of the Central Asian Orogenic Belt. J Geol Soc Lond 164:31–47

Wu T, He G (1992) Ophiolitic melange belts in the northern margin of the Alashan Block. J Grad Sch China Univ Geosci 6:286–296 **(in Chinese with English abstract)**

Wu T, He G (1993) Tectonic units and their fundamental characteristics on the northern margin of the Alxa block. Acta Geol Sin 67:97–108 **(in Chinese with English abstract)**

Wu T, He G, Zhang C (1998) On Palaeozoic Tectonics in the Alxa Region, Inner Mongolia, China. Acta Geol Sin 72:256–263

Wu F, Jahn BM, Wilde S, Lo C, Yui T, Lin Q, Ge W, Sun D (2003) Highly fractionated I-type granites in NE China (II): isotopic geochemistry and implications for crustal growth in the Phanerozoic. Lithos 67:191–204

Xiao W, Windley B, Huang B, Han C, Yuan C, Chen H, Sun M, Sun S, Li J (2009a) End-Permian to mid-Triassic termination of the accretionary processes of the southern Altaids: implications for the geodynamic evolution, Phanerozoic continental growth, and metallogeny of Central Asia. Int J Earth Sci 98:1189–1217

Xiao W, Windley B, Yuan C, Sun M, Han C, Lin S, Chen H, Yan Q, Liu D, Qin K, Li J, Sun S (2009b) Paleozoic multiple subduction-accretion processes of the Southern Altaids Ameriacan. J Sci 309:221–270

Xiao W, Windley BF, Allen MB, Han C (2013) Paleozoic multiple accretionary and collisional tectonics of the Chinese Tianshan orogenic collage. Gondwana Res 23:1316–1341

Yang QD, Zhang L, Wang T, Shi XJ, Zhang JJ, Tong Y, Guo L, Geng JZ (2014) Geochemistry and LA-ICP-MS zircon U-Pb age of Late Carboniferous Shalazhashan pluton on the northern margin of the Alxa Block, Inner Mongolia and their implications. Geol Bull China 33:776–787

Zen E (1988) Phase relations of peraluminous granitic rocks and their petrogenetic implications. Annu Rev Earth Planet Sci 16:21–51

Zhang W (2013) Late Paleozoic granitoids in Beishan-northern Alxa area (NW China) and their tectonic implications. PhD thesis, Peking University (in Chinese with English abstract)

Zhang J, Li J, Liu J, Feng Q (2011) Detrital zircon U–Pb ages of Middle Ordovician flysch sandstones in the western ordos margin: new constraints on their provenances, and tectonic implications. J Asian Earth Sci 42:1030–1047

Zhang J, Wang T, Zhang Z, Tong Y, Zhang L, Shi X, Guo L, Li S, Zeng T (2012) Magma mixing origin of Yamatu Granite in Nuoergong—Langshan Area, Western Part of the Northern Margin of North China Craton: petrological and geochemical evidences. Geol Rev 58:53–66 **(in Chinese with English abstract)**

Zhang W, Wu T, Feng J, Zheng R, He Y (2013a) Time constraints for the closing of the Paleo-Asian Ocean in the Northern Alxa

Region: evidence from Wuliji granites. Sci China Earth Sci 56:153–164

Zhang L, Shi X, Zhang J, Yang Q, Tong Y, Wang T (2013b) LA–ICP–MS zircon U–Pb age and geochemical characteristics of the Taohaotuoxiquan gabbro in northern Alxa, Inner Mongolia. Geol Bull China 32:1536–1547 **(in Chinese with English abstract)**

Zhang W, Pease V, Meng Q, Zheng R, Thomsen TB, Wohlgemuth-Ueberwasser C, Wu T (2015) Discovery of a Neoproterozoic granite in the Northern Alxa region, NW China: its age, petrogenesis and tectonic significance. Geol Mag. doi:10.1017/S0016756815000631

Zhao G, Sun M, Wilde S, Sanzhong L (2005) Late Archean to paleoproterozoic evolution of the North China Craton: key issues revisited. Precambrian Res 136:177–202

Zheng R, Wu T, Zhang W, Feng J, Xu C, Meng Q, Zhang Z (2013) Geochronology and geochemistry of the Yagan granite in the northern margin of the Alxa block: constraints on the tectonic evolution of the southern Altaids. Acta Petrol Sin 29:2665–2675 **(in Chinese with English abstract)**

Zheng R, Wu T, Zhang W, Xu C, Meng Q, Zhang Z (2014) Late Paleozoic subduction system in the northern margin of the Alxa block, Altaids: geochronological and geochemical evidences from ophiolites. Gondwana Res 25:842–858

Zhu DC, Mo XX, Wang XX, Zhao ZD, Niu Y, Zhou CY, Yang YH (2009) Petrogenesis of highly fractionated I-type granites in the Zayu area of eastern Gangdese, Tibet: constraints from zircon U–Pb geochronology, geochemistry and Sr–Nd–Hf isotopes. Sci China Ser D Earth Sci 52:1223–1239